

# POLYMER SHAPE DYNAMICS INDUCED BY SPATIALLY CORRELATED NOISE\*

M. MAJKA<sup>†</sup>, P.F. GÓRA

The Marian Smoluchowski Institute of Physics  
and

The Mark Kac Complex Systems Research Center  
Jagiellonian University, Reymonta 4, 30-059 Kraków, Poland

*(Received April 23, 2012)*

In this paper, we examine the influence of a spatially correlated noise on a 2D polymer-like particle. The molecule is modeled with harmonic potential for bonds and angular interactions and a global Lennard–Jones potential. We present a method for generating a spatially correlated noise if the time and spatial terms in the correlation function factorize. The dynamics of polymer’s shape transformation process is investigated by means of Fourier analysis. An increase in correlation length results in the environmentally induced stiffening of the chain.

DOI:10.5506/APhysPolB.43.1133

PACS numbers: 05.40.Ca, 36.20.–r

## 1. Introduction

The noise-induced behavior of molecules has been intensively researched on over the past two decades in the context of biophysics, as it seems crucial for the understanding of the intracellular transport and conformation transitions in bioparticles. The attention of researchers is currently drawn by phenomena like sub-diffusion which has been recently related to the temporal correlations in the thermal noise [1]. However, while the presence of white or time-correlated noise can lead to a spatiotemporal order in a variety of systems [2, 3], little is known about the effects that arise from the spatial organization of the noise itself. Therefore, in our work, we have focused on the influence of a Gaussian noise with purely spatial correlations (SCGN) on the shape of a long polymer-like particle.

---

\* Presented at the XXIV Marian Smoluchowski Symposium on Statistical Physics, “Insights into Stochastic Nonequilibrium”, Zakopane, Poland, September 17–22, 2011.

<sup>†</sup> [maciej.majka@uj.edu.pl](mailto:maciej.majka@uj.edu.pl)

We have developed a 2D model of such a molecule, characterized by multiple and well-localized energy minima that relate to the numerous possible shapes of the polymer chain. Then, the time evolution of such a system has been simulated, under the forcing of SCGN, to examine whether the transduction between energy minima (thus, the chain's shape as well) is affected by the spatially structured noise as compared to the case of uncorrelated random forcing. For a range of correlation lengths  $\lambda$  and noise amplitudes  $kT$ , we have gathered data regarding the shape coefficient and analyzed the asymptotic behavior of its power density spectra.

The paper is organized as follows: first, in Section 2 we briefly discuss the method of spatially correlated noise generation ; in Section 3 we present our 2D model of polymer-like particle; in Section 4 we define the shape coefficient, which has been measured in our simulations; Section 5 covers our simulation methodology; the Fourier analysis of our data is discussed in Section 6; Section 7 summarizes our results.

## 2. Generation of SCGN

Let us define two Gaussian variables  $\xi_i$  and  $\eta_i$ , correlated in the following manner

$$\langle \eta_i \eta_j \rangle = \delta_{ij}, \quad (1)$$

$$\langle \xi_i \xi_j \rangle = S_{ij}. \quad (2)$$

The Eq. (2) defines a symmetric and positively defined correlation matrix  $\hat{S}$ , whose matrix elements are equal to  $(\hat{S})_{ij} = S_{ij}$ . To obtain a vector of  $N$  correlated variables  $\vec{\xi}^T = (\xi_1, \dots, \xi_i, \dots, \xi_N)^T$  from an uncorrelated vector  $\vec{\eta}^T = (\eta_1, \dots, \eta_i, \dots, \eta_N)^T$ , first one must find the Cholesky decomposition of matrix  $\hat{S}$

$$\hat{S} = \hat{L} \hat{L}^T. \quad (3)$$

Here  $\hat{L}$  is a lower triangular matrix. Generating  $\vec{\xi}$  from  $\vec{\eta}$  requires calculating

$$\vec{\xi} = \hat{L} \vec{\eta}. \quad (4)$$

The above algorithm can be also found in [4].

In our simulation, the variable  $\xi_i$  is the function of both time  $t$  and position  $\vec{r}_i$  (namely,  $\xi_i(t) = \xi(\vec{r}_i, t)$ ) that represents a stochastic, yet spatially structured forcing driving a Langevin particle. Therefore, we assume the spatial and temporal parts of its correlation function to factorize and we have chosen this function to be

$$\langle \xi(\vec{r}_i, t) \xi(\vec{r}_j, t') \rangle = S_{ij}(t) = \frac{2kT\gamma}{m} e^{-\frac{|\vec{r}_i - \vec{r}_j|}{\lambda}} \delta(t - t'). \quad (5)$$

In Eq. (5)  $k$  is the Boltzmann constant,  $T$  stands for temperature,  $\gamma$  denotes the friction coefficient,  $m$  is a particle mass, and  $\lambda$  refers to a correlation length. The norming factor is chosen in such a way that for  $\lambda \rightarrow 0$  it is in agreement with the Brownian diffusion.

To numerically solve a  $\xi_i(t)$ -dependent differential equation, one has to perform a Cholesky decomposition of the matrix  $\hat{S}(t)$  for every integration step, as  $\hat{S}(t)$  depends on current positions  $\vec{r}_i(t)$ . These frequent decompositions are the most computationally expensive part of our simulation.

Additionally, our model is two-dimensional, which means that one has to find a vector  $(\xi_{x,i}(t), \xi_{y,i}(t))^T$  for every position  $\vec{r}_i(t)$ . For the sake of simplicity, we assume the  $x$  component to be independent from the  $y$  component, which allows us to generate them independently.

In the Fig. 1, a result of a single generation procedure for the regular network is presented. There is a distinct pattern of ordered clusters for the correlated noise and no regularities for the non-correlated one. However, this pattern of clusters changes entirely for different  $\vec{\eta}$ .

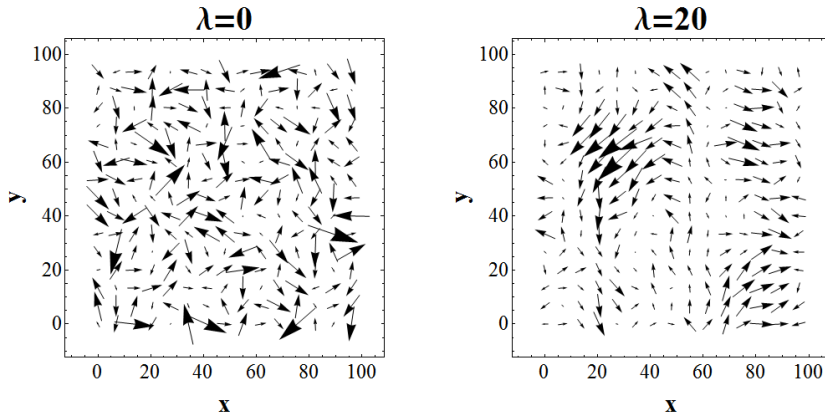


Fig. 1. The comparison between snapshots of vector field  $\vec{\xi}(\vec{r}_i, t)$  for regular network.

### 3. The model of 2D polymer-like molecule

Our model is based on bead-spring approach, yet extended to two dimensions (so  $\vec{r}_i^T = (x_i, y_i)^T$ ), and supplied with angular interactions to provide bending of chains and Lennard-Jones interaction that introduce excluded volume. The bonds between beads  $i$ th and  $(i+1)$ th are modeled with harmonic potential

$$U_{R,i} = \frac{1}{2} k_R (|\vec{r}_{i+1} - \vec{r}_i| - d_0)^2. \quad (6)$$

The angular interaction results from harmonic potential applied to beads  $i$ th and  $(i+2)$ th

$$U_{\psi,i} = \frac{1}{2}k_{\psi}(|\vec{r}_{i+2} - \vec{r}_i| - l_0)^2. \quad (7)$$

The Lennard–Jones interactions are applied between every two beads

$$U_{\text{LJ},ij} = \epsilon \left( \frac{\sigma^{12}}{|\vec{r}_i - \vec{r}_j|^{12}} - \frac{\sigma^6}{|\vec{r}_i - \vec{r}_j|^6} \right). \quad (8)$$

The resultant potential for  $N$  beads reads

$$U = \sum_{i=1}^{N-1} U_{\text{R},i} + \sum_{i=1}^{N-2} U_{\psi,i} + \frac{1}{2} \sum_{i=1, j=1}^{N,N} U_{\text{LJ},ij}. \quad (9)$$

With the Lennard–Jones interactions switched off ( $\epsilon = 0$ ), the geometry that minimizes energy is given by conditions

$$\begin{cases} |\vec{r}_{i+1} - \vec{r}_i| = d_0, \\ |\vec{r}_{i+2} - \vec{r}_i| = l_0. \end{cases} \quad (10)$$

If positions of  $(i+1)$ th and  $i$ th satisfy the relation  $|\vec{r}_{i+1} - \vec{r}_i| = d_0$ , there are always two equivalent possibilities to chose  $\vec{r}_{i+2}$ , so the Eq. (10) is fulfilled. For  $N$  beads, this ambiguity leads to  $2^{N-3}$  different chain shapes for the even  $N$ , and  $2^{N-3} + 2^{N/2-2}$  for the odd  $N$ . All of these conformations have the same energy, equal to 0.

Introducing the  $U_{\text{LJ},ij}$  disturbs the condition (10), but the numerical investigation shows that a general rule of two possible bead's positions that minimize the energy remains valid for a wide range of potentials' parameters. However, these conformations are no longer equienergetic.

An effective potential well that a single bead moves in can be easily visualized when  $i$ th bead's 4 nearest neighbors are taken into consideration. Having analyzed the resultant energy landscape, we have chosen the parameters of potential (Table I) so the effective well has 2 distinct minima for most of local geometries. Fig. 2 illustrates the energy map for the chosen parameters. We have analyzed the influence of local geometry disturbances on the energy landscape. While changing angles between bonds leads to an asymmetry in minima depth, this effect seems to be insignificant in comparison to the decrease of energy barrier resulting from local stretching of the polymer (Fig. 3), which can easily facilitate the process of conformation transition.

TABLE I

The parameters of the model chosen for simulation. The bracket for  $k_\psi$  indicates two values investigated.

Parameter	$N$	$m$	$k_R$	$d_0$	$k_\psi$	$l_0$	$\epsilon$	$\sigma$	$\gamma$
Value	40	1	1	5	5(1)	8	5	4.85	5

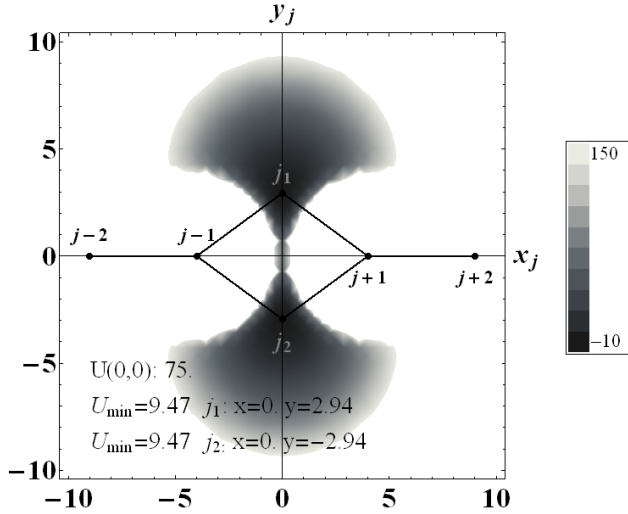


Fig. 2. Energy landscape for a single bead. The parameters of potential have been chosen according to Table I, with  $k_\psi = 5$ . Points  $j - 2$  to  $j + 2$  reassemble the local geometry of chain.  $j_1$  and  $j_2$  are the two possible positions of  $j$ th bead that minimize energy.  $U_{\min}$  and  $U(0,0)$  denotes minimum energy and the height of energy barrier, respectively.

Having determined the potential  $U$ , the chain dynamics is govern by the following system of  $2N$  equations of motion

$$\begin{cases} \ddot{x}_i + \gamma \dot{x}_i + \partial_{x_i} U = \xi_x(\vec{r}_i, t) , \\ \ddot{y}_i + \gamma \dot{y}_i + \partial_{y_i} U = \xi_y(\vec{r}_i, t) . \end{cases} \quad (11)$$

In Eq. (11) the coefficient  $\gamma$  is the friction constant,  $\xi_x(\vec{r}_i, t)$  and  $\xi_y(\vec{r}_i, t)$  are SCGNs, bead mass is assumed to be equal 1.

The equations (11) describe both the inertial and dissipative dynamics of the system, but we have investigated only the over-damped regime by choosing relevant parameters. However, the inertial terms have not been neglected entirely, to provide a better accuracy.

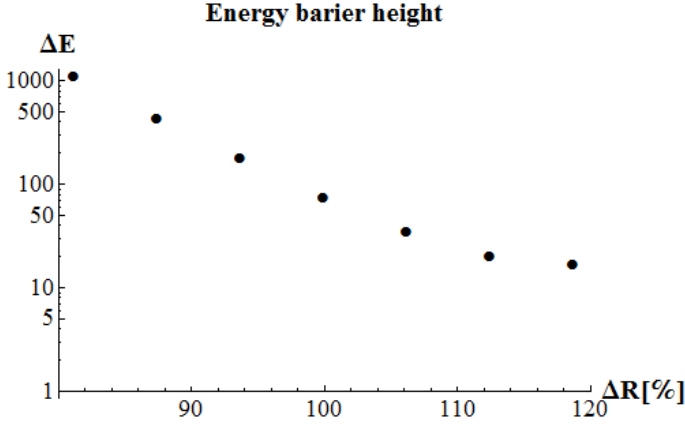


Fig. 3. The influence of chain extension on the energy barrier height,  $\Delta E = U(0, 0) - U_{\min}$  and  $\Delta R = |\vec{r}_{j+1} - \vec{r}_{j-1}|/l_0$ .

#### 4. Shape coefficient

The previous section emphasizes that for the proposed (Table I) parameters set, every bead has two positions that minimize the energy, which are separated by a potential barrier. Hence, when a fluctuation–dissipation feedback is provided to the system by the stochastic forcing and the friction, the chain geometry is going to fluctuate near one of the minima, occasionally taking transition to another minimum. We identify these jumps as conformational transitions. Thus, in order to track such events, it is convenient to systematically describe a current chain shape by the sequence of numbers  $\kappa_i = \pm 1$  indicating the chain's bending direction at  $i$ th site.

To determine  $\kappa_i$  one has to perform the following transformation

$$\left\{ \begin{array}{ll} \Delta \vec{r}_i = \vec{r}_i - \vec{r}_{i-1} = (\Delta x_i, \Delta y_i)^T, \\ \phi = -\arccos \frac{\Delta x_i}{|\Delta \vec{r}_i|} & \text{if } \Delta y_i > 0, \\ \phi = -\left(2\pi - \arccos \frac{\Delta x_i}{|\Delta \vec{r}_i|}\right) & \text{if } \Delta y_i \leq 0, \\ \vec{r}_{i+1} = \hat{R}(\phi) (\vec{r}_{i+1} - \vec{r}_{i-1}). \end{array} \right. \quad (12)$$

In Eq. (12) the matrix  $\hat{R}(\phi)$  performs a rotation about a given angle  $\phi$ . Once the  $\vec{r}'_{i+1} = (x'_{i+1}, y'_{i+1})^T$  is found, the  $\kappa_i$  value is chosen according to the following rules

$$\begin{array}{ll} y'_{i+1} > 0 & \Rightarrow \kappa_i = 1, \\ y'_{i+1} < 0 & \Rightarrow \kappa_i = -1. \end{array} \quad (13)$$

The series of  $\kappa_i$  for  $i = 2, \dots, N - 1$  completely determines the minimum energy structure that the chain geometry is closest to. However, as we are interested in the dynamics of shape transformation process, let us define the shape coefficient  $K$ , equal to the absolute value of the average bending direction

$$K = \frac{1}{N} \left| \sum_{i=2}^{N-1} \kappa_i \right|. \quad (14)$$

The coefficient  $K \approx 0$  indicates that there is approximately the same number of positive and negative  $\kappa_i$ , while there is  $0 < K < 1$  if one of the bending directions predominates.

In the light of Eq. (14),  $K(t)$  represents the time evolution of the bending direction surplus, thus providing the collective description of chain shape. The short-time behavior is strictly dependent on the number of conformation transitions that occurred between two measurements, at  $K(t)$  and  $K(t + \Delta t)$ , assuming that this period is short enough that there is only a limited number of transitions during  $\Delta t$ . Hence, the short time regime informs us about the susceptibility of the polymer conformation to disturbances inflicted by the noise.

## 5. Simulation methods

In order to examine the  $K(t)$  dependence on  $\lambda$  and  $kT$ , we have simulated the time evolution of the system described by Eq. (11), using parameters from Table I. For the numerical solution of Eq. (11), we have applied the classical 4th order Runge–Kutta method modified for stochastic differential equations [5], with an integration time step equal to  $1/128$  time units. While we are not interested in inertial effects introduced by  $\ddot{x}_i$  and  $\ddot{y}_i$ , we have set  $\gamma = 5$ , which is enough to over-damp the system. Additionally, to enhance equilibration process, which occurs at the beginning of each run, we have temporally increased  $\gamma$  to 10 units and returned to its standard value after 25 time units.

The cases of strong ( $k_\psi = 5$ ) and weak ( $k_\psi = 1$ ) angular interaction have been investigated. We have collected data of  $K(t)$  for the correlation lengths ranging from  $\lambda = 0$  to 20 units and  $kT = 2$  to 12 units, increasing these parameters at 5 and 2 units intervals respectively and repeating simulations 40 times for each pair of  $\lambda$  and  $kT$ , to provide reliable statistics. During each run, which has been started with different initial positions, the  $K(t)$  values have been registered for 1124 time units at the step of 1 unit, with first 100 units rejected from further analysis for the reason of system equilibration.

## 6. Fourier analysis of the $K(t)$

The Power Density Spectrum (PDS) of  $K(t)$  reveals the contribution of high and low frequencies in the shape transformation process. To obtain a quantitative measure of the  $\lambda$  and  $kT$  influence on conformation transitions dynamics, we have approximated the asymptotic behavior of PDS by the power-law function. Using  $A(\omega)$  to denote an averaged PDS spectrum, we assume

$$A(\omega) \xrightarrow{\omega \rightarrow +\infty} \omega^\alpha. \quad (15)$$

The Fourier Transformation of  $K(t)$  has been performed to obtain the PDS from each run. These PDS have been mean-valued for corresponding  $\lambda$  and  $kT$ , log-log scaled and a linear function  $\alpha \ln \omega + C$  has been fitted to their high frequency tails ( $\omega > 0.05$ ). In all cases, the regression error for  $\alpha$  was lower than  $\Delta\alpha = \pm 0.005$  and the coefficient of determination  $R^2$  has been included in a range  $0.89 \leq R^2 \leq 0.93$ .

The averaged PDS are presented in Fig. 4. The data for both  $k_2 = 5$  and  $k_2 = 1$  are qualitatively similar, being most divergent for  $\lambda = 0$ .

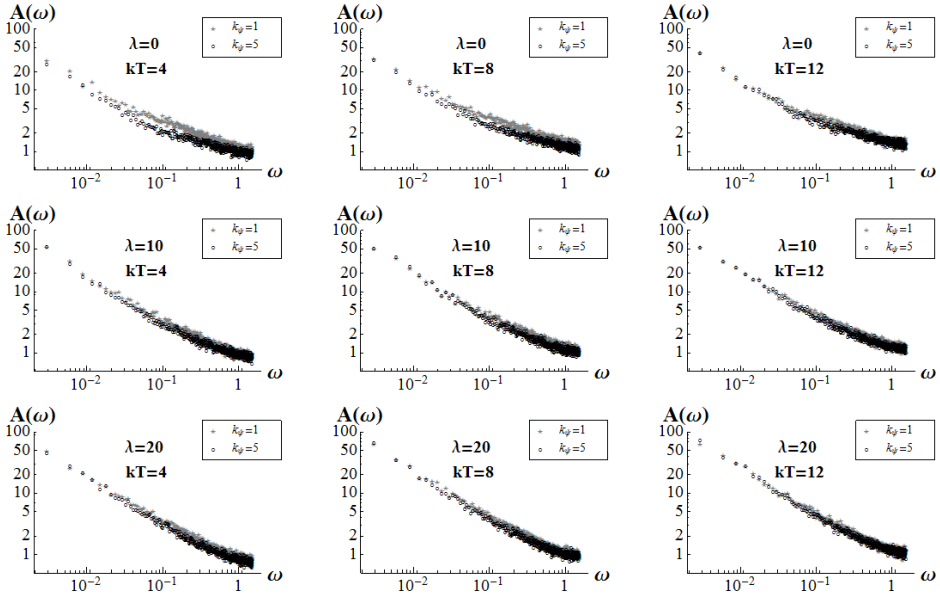


Fig. 4. The representative selection of mean-valued PDS.

The obtained  $\alpha(\lambda, kT)$  are illustrated in Fig. 5. It is evident that  $\alpha$  is falling as there is an increase in  $\lambda$ , for both  $k_2 = 5$  and  $k_2 = 1$ . However, while for  $k_2 = 5$  the  $\alpha(\lambda = \text{const.}, kT)$  varies insignificantly with the rise in  $kT$ , the analogical dependence for  $k_2 = 1$  tends to grow distinctly with  $kT$  for lower  $\lambda$ , but this effect attenuates as  $\lambda$  elongates.



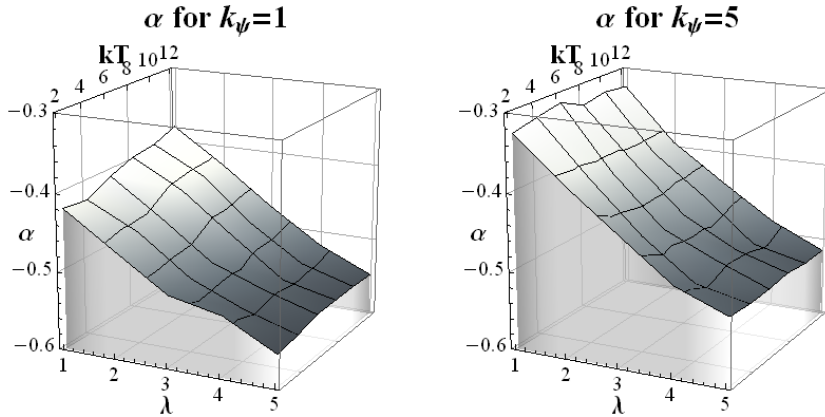


Fig. 5. The values of exponents  $\alpha$  plotted against its parameters.

## 7. Interpretation

As stated above, the short-time behavior of  $K(t)$ , which is strictly related to the conformation transitions rate, is governed by high frequencies in PDS. Therefore, the exponent  $\alpha$ , being a straightforward measure of this high frequency contribution, reflects the fact, that the presence of spatial correlations in the thermal noise lowers the number of conformation transitions per time unit. Additionally, the non-zero  $\lambda$  makes this rate less sensitive to the temperature growth, however this effect depends on the angular interaction strength.

The decline in conformation transition rate can be understood as an environmentally induced stiffening of the chain. Its dependence on  $\lambda$  comes as no surprise, as the noise within  $\lambda$  range is effectively invariant, so the subsections of the chain shorter than  $\lambda$  experience almost no relative forcing and so their shape is conserved. However, at the length scale larger than  $\lambda$  these parts still move in an uncorrelated manner that leads to the local geometry disturbances and results in conformational transitions.

Our simulations indicate that the externally introduced spatial correlations in the thermal noise affect the system that is subjected to it. However, the other aspects of this interaction and its physical justification require further investigation. Especially, the physically valid formula for spatiotemporal correlation function, derived from microscopic consideration, is yet to be identified. However, we have shown that the effective means to simulate these kinds of systems are available, providing that the spatial and temporal parts of the correlation function factor out.

## REFERENCES

- [1] S.C. Kou, *Ann. Appl. Stat.* **2**, 501 (2008).
- [2] F. Sagués, J.M. Sancho, J. García-Ojalvo, *Rev. Mod. Phys.* **79**, 829 (2007).
- [3] R. Morgado, M. Cieřła, L. Longa, F.A. Oliveira, *Europhys. Lett.* **79**, 10002 (2007).
- [4] R. Wieczorkowski, R. Zieliński, *Komputerowe Generatory Liczb Losowych*, WNT, Warszawa 1997 (in Polish).
- [5] P.E. Kloeden, E. Platen, *Numerical Solutions of Stochastic Differential Equations*, Springer-Verlag, Berlin 1992.